Absorption and emission properties of Nd^{3+} in lithium cesium mixed alkali borate glasses

Y.C. Ratnakaram[a,*], A. Vijaya kumar[a], D. Tirupathi Naidu[a], R.P.S. Chakradhar[b]

[a]*Department of Physics, S.V.University Post Graduate Centre, Kavali 524 201, AP, India*
[b]*Department of Physics, Indian Institute of Science, Bangalore 560012, Karnataka, India*

Abstract

Lithium cesium mixed alkali borate glasses of the composition $67B_2O_3 \cdot xLi_2O \cdot (32-x)Cs_2O$ (where $x = 8$, 12, 16, 20 and 24) containing 1 mol% Nd_2O_3 were prepared by melt quenching. The absorption spectra of Nd^{3+} were studied from the experimental oscillator strengths and the Judd–Ofelt intensity parameters were obtained. The intensity parameters are used to determine the radiative decay rates (emission probabilities of transitions) (A_T), branching ratios (β) and integrated absorption cross-sections (Σ) of the Nd^{3+} transitions from the excited state J manifolds to the lower lying J' manifolds. Radiative lifetimes (τ_R) are estimated for certain excited states of Nd^{3+} in these mixed alkali borate glasses. Luminescence spectra were measured and the emission cross-sections (σ_p) were evaluated for the three emission transitions. The variation of luminescence intensity with x was recorded for the three transitions at different excitation power to see the effect of mixed alkalies in these borate glasses.

1. Introduction

Optical properties like optical absorption and luminescence spectra of various rare earth (RE) ions doped alkali and mixed alkali borate glasses have been extensively investigated in the recent years [1–5]. Glasses doped with trivalent rare earth neodymium ion have become important optical materials for use in the field of lasers and optical wave-guides. A lot of research work has been reported during the past few years on the spectroscopic and lasing properties of Nd^{3+} doped glasses, because it is easy to prepare and synthesize large sized samples than to grow crystals [6–10]. The effect of host matrix on the local environment of a given RE cation with its first nearest neighbor anions such as oxygen can be elucidated using Judd–Ofelt theory [11,12]. For alkali borate glasses, the abrupt property changes were observed between 15 and 20 mol% modifier oxide [13]. This peculiar and anomalous behavior referred to as 'borate anomaly' and it was first explained in terms of the unique ability of boron to exist in two distinct co-ordination states-the trigonal and tetrahedral states. The addition of alkali oxide to boric oxide results in the conversion of boron from trigonal to tetrahedral co-ordination and at 20 mol% of R_2O (R = alkali ion) the tetraborate reaches maximum concentration, the boroxyl group disappears and the formation of diborate starts.

Many physical properties of the oxide glasses containing alkali oxide as a modifier show non-linear behavior if the alkali ion is gradually replaced by another alkali ion,

---

* Corresponding author. Tel.: +91 8626 244271; fax: +91 244 271.

E-mail address: ratnakaram_yc@yahoo.co.in
(Y.C. Ratnakaram).

keeping the total alkali content constant. This non-linear behavior as a function of relative alkali content is known as the mixed alkali effect (MAE) [14]. In the recent past, we have studied the spectroscopic investigations of Nd^{3+} in lithium sodium and lithium potassium [15] mixed alkali borate glasses. In the present work, we report the spectroscopic and laser properties of Nd^{3+} doped lithium cesium mixed alkali borate glasses of the type $67B_2O_3 \cdot xLi_2O \cdot (32-x)Cs_2O$ (where $x = 8$, 12, 16, 20 and 24). Our main thrust of the present work is on examining the effect of mixed alkalies (lithium, cesium) on the spectroscopic properties of Nd^{3+} doped borate glasses by studying the variation in Judd–Ofelt intensity parameters, radiative lifetimes and emission cross-sections with x in the above glass matrix.

2. Experimental details

The Nd^{3+} doped lithium cesium mixed alkali borate glasses were prepared using appropriate amounts of H_3BO_3, Li_2CO_3, Cs_2CO_3 and Nd_2O_3. These raw materials were thoroughly mixed and melted in the range of 950–1100 °C. The melt was air quenched between two well-polished brass plates. The samples were annealed at 200 °C for 2–3 h to remove thermal strains. The details of the preparation of these glass systems and the other measurements are given in our earlier article [15].

The systems studied in the present work are $67B_2O_3 \cdot 8Li_2O.24Cs_2O \cdot 1Nd_2O_3$ ($x = 8$), $67B_2O_3 \cdot 12Li_2O \cdot 20Cs_2O \cdot 1Nd_2O_3$ ($x = 12$), $67B_2O_3 \cdot 16Li_2O \cdot 16Cs_2O \cdot 1Nd_2O_3$ ($x = 16$), $67B_2O_3 \cdot 20Li_2O \cdot 12Cs_2O \cdot 1Nd_2O_3$ ($x = 20$) and $67B_2O_3 \cdot 24Li_2O \cdot 8Cs_2O \cdot 1Nd_2O_3$ ($x = 24$). Optical absorption spectra of the polished samples were recorded at room temperature using U3400 spectrophotometer. Luminescence spectra were obtained at room temperature using Midac-FT photoluminescence spectrophotometer under excitation wavelength 514 nm of Ar^{3+} laser. The refractive indices of the samples were determined with an Abbe refractometer using monobromonaphthalene as an adhesive coating with an accuracy of ± 0.001 and the density measurements were made using Archimedes principle with xylene as immersion liquid to ± 0.02 g/cm³. The sample thicknesses were obtained using a micrometer to ± 0.002 cm.

3. Results and discussion

3.1. Intensity parameters

The room temperature optical absorption spectra of Nd^{3+} doped lithium cesium mixed alkali borate glasses in the range 390–900 nm are shown in Fig. 1 for different x values in the glass matrix. Though the observed spectra appear similar for different compositions, the spectral intensities and the shape of the spectral profiles of certain
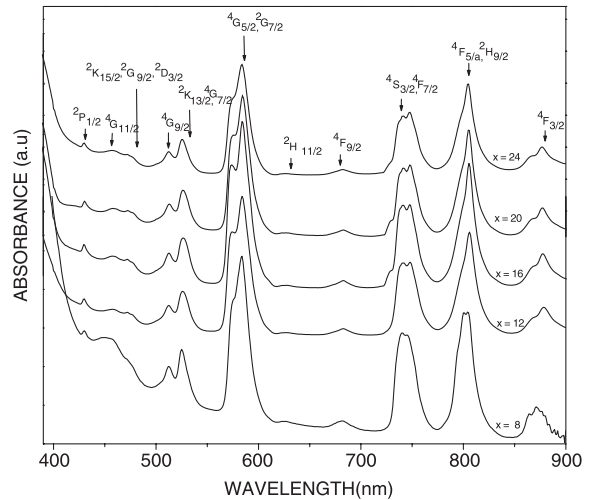

Fig. 1. Optical absorption spectra of Nd^{3+} in $67B_2O_3 \cdot xLi_2O \cdot (32-x)Cs_2O$ ($x = 8$, 12, 16, 20 and 24) glasses.

transitions vary. The best set of Judd–Ofelt intensity parameters (Ω_2, Ω_4 and Ω_6) obtained from a least square analysis of the observed oscillator strengths are presented in Table 1 for all the glass matrices. The Judd–Ofelt intensity parameters in binary borate glasses and lithium sodium, lithium potassium mixed alkali borate glasses are also presented in the table. These parameters depend on the host glass composition [2]. Judd–Ofelt parameter, Ω_2 in particular, increases with the increase in covalency of the bond between the rare earth ion and the ligand anions. It is observed in the present work that Ω_2 parameter increased when the third component, cesium is added to the lithium borate glass. It indicates increase in covalency and asymmetry of the local environment of rare earth ion in this mixed alkali borate glass [16]. Ω_2 parameter is maximum at $x = 12$ mol% in lithium cesium glass matrix among the three mixed alkali borate glasses indicating strong covalency and more asymmetry at this composition. According to Oomen and van Dongen [17], the sum of Judd–Ofelt intensity parameters $\Sigma \Omega_\lambda$ also increases with the increase in covalency. These values are also presented in Table 1 for all the glass matrices. From the table it is observed that $\Sigma \Omega_\lambda$ values are decreasing (considering experimental error in the intensity parameters) with the increase in x which indicate decrease in covalency and asymmetry of the local environment of the rare earth ion with the decrease in cesium content in the glass matrix. From the table it is also observed that $\Sigma \Omega_\lambda$ values are nearly equal at $x = 8$ and 12 mol% and they are large indicating strong covalency. Similarly these values are nearly equal for $x = 20$ and 24 mol% and they are small indicating weak covalency. Ω_6 parameter is maximum at $x = 8$ mol% which indicates more rigidity of the host material at this composition.

$^4I_{9/2} \rightarrow {}^4G_{5/2} + {}^2G_{7/2}$ is the hypersensitive transition for Nd^{3+} ion [18]. It follows the selection rules $\Delta J \leq 2$, $\Delta L \leq 2$,

Table 1
Judd–Ofelt intensity parameters ($\Omega_\lambda \times 10^{20}$) (cm^2) and peak intensity ratios (I_L/I_S) of hypersensitive transition of Nd^{3+} doped lithium cesium mixed alkali borate glasses

S. No	Glass matrix	Ω_2	Ω_4	Ω_6	$\sum \Omega_\lambda$	I_L/I_S	Reference
1	$8Li_2O + 24Na_2O + 67B_2O_3$	8.81 ± 0.78	6.78 ± 0.68	9.01 ± 0.88	24.60 ± 2.42	–	[15]
2	$12Li_2O + 20Na_2O + 67B_2O_3$	9.59 ± 0.92	7.87 ± 0.72	9.84 ± 0.98	27.32 ± 2.63	–	[15]
3	$16Li_2O + 16Na_2O + 67B_2O_3$	8.39 ± 0.75	6.51 ± 0.61	10.01 ± 1.04	24.92 ± 2.32	–	[15]
4	$20Li_2O + 12Na_2O + 67B_2O_3$	7.57 ± 0.69	7.01 ± 0.67	8.86 ± 0.82	23.45 ± 2.13	–	[15]
5	$24Li_2O + 8Na_2O + 67B_2O_3$	8.53 ± 0.82	7.47 ± 0.70	9.60 ± 0.87	25.61 ± 2.22	–	[15]
6	$8Li_2O + 24K_2O + 67B_2O_3$	7.94 ± 0.77	3.57 ± 0.28	7.94 ± 0.78	19.45 ± 1.66	1.032	[15]
7	$12Li_2O + 20K_2O + 67B_2O_3$	10.83 ± 0.93	7.73 ± 0.74	9.04 ± 0.86	27.61 ± 2.52	1.091	[15]
8	$16Li_2O + 16K_2O + 67B_2O_3$	10.28 ± 0.89	8.12 ± 0.78	10.58 ± 0.96	28.98 ± 2.64	1.113	[15]
9	$20Li_2O + 12K_2O + 67B_2O_3$	11.08 ± 1.03	8.92 ± 0.84	11.57 ± 1.05	31.49 ± 2.87	1.123	[15]
10	$24Li_2O + 8K_2O + 67B_2O_3$	11.52 ± 1.06	9.55 ± 0.91	13.62 ± 1.25	34.69 ± 3.32	1.230	[15]
11	$8Li_2O + 24Cs_2O + 67B_2O_3$	15.48 ± 1.42	10.36 ± 0.88	19.40 ± 1.87	45.24 ± 3.96	–	Present work
12	$12Li_2O + 20\ Cs_2O + 67B_2O_3$	18.40 ± 1.64	10.28 ± 0.76	16.65 ± 1.55	45.33 ± 3.52	1.180	Present work
13	$16Li_2O + 16\ Cs_2O + 67B_2O_3$	11.46 ± 0.98	6.37 ± 0.62	9.53 ± 0.92	27.36 ± 2.65	1.126	Present work
14	$20Li_2O + 12\ Cs_2O + 67B_2O_3$	9.97 ± 0.91	6.18 ± 0.55	9.39 ± 0.87	25.54 ± 2.44	–	Present work
15	$24Li_2O + 8\ Cs_2O + 67B_2O_3$	10.24 ± 0.89	5.53 ± 0.43	10.05 ± 0.78	25.82 ± 2.67	–	Present work
16	$30Na_2O + 70B_2O$	4.91	3.28	4.51	12.70	–	[22]
17	$30K_2O + 70B_2O$	4.94	3.10	3.42	11.46	–	[22]
18	$30Li_2O + 70B_2O$	4.20	3.89	4.74	12.83	–	[22]

and $\Delta S = 0$. The position and intensity of the hypersensitive transition are very sensitive to the environment of the rare earth ion. In the present work, there is no change in the position of the peak wavelength of the hypersensitive transition with x. Judd [19] suggested that the spectral profile of the hypersensitive transition is strongly affected by changes in the symmetry of the crystal field acting on the rare earth ion. A difference in the shape of the transition indicates a difference in the environment of the Nd^{3+} ion. The spectral profiles of the hypersensitive transition for different x values in the glass matrix are shown Fig. 2. In the present work, it is observed that the spectral profiles of the hypersensitive transition is different for different x values in the glass matrix indicating significant differences in the crystal field asymmetries. The Stark splitting due to crystal field splits the hypersensitive transition in the absorption spectra into two peaks. The peak intensity ratios of the longer and shorter wavelength components are designated as I_L/I_S. An increase in the intensity ratio indicates a shift of the center of gravity of the absorption spectra to longer wavelength [20], which indicates an increase in covalency of Nd–O bond. In the present work, the Stark splitting of the $^4I_{9/2} \rightarrow {}^4G_{5/2} + {}^2G_{7/2}$ transition is not resolved for $x = 8$ mol%. There is clear splitting for $x = 12$ and 16 mol% and the peak intensity ratios are 1.180 and 1.126 which indicates more covalency at $x = 12$ mol% and less covalency at $x = 16$ mol%. For $x = 20$ and 24 mol% the splitting is decreased and the relative intensities of the components changed, so that the splitting is hidden by the inhomogeneous broadening. It indicates structural changes at $x = 16$–20 mol% and at $x = 20$–24 mol%. In the case of lithium sodium glass, the hypersensitive transition is not resolved for all the x values. For lithium potassium glass, there is clear splitting for $x = 8$, 12 and 16 mol% and the splitting is decreased at $x = 20$ and

24 mol% [15]. Ω_λ can also be written as

$$\Omega_\lambda = (2t + 1) \sum_{s,p} |A_{s,p}|^2 \Xi^2(s, t)(2s + 1)^{-1},$$
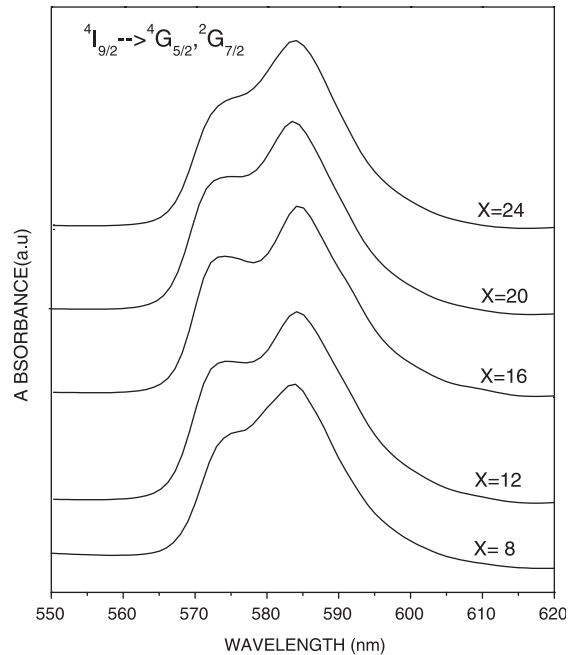
(1)

$t = 2, 4, 6$

Fig. 2. Variation of spectral profiles of the hypersensitive transition, $^4I_{9/2} \rightarrow {}^4G_{5/2}$, $^2G_{7/2}$ with x in lithium cesium mixed alkali borate glasses.

where $A_{s,p}$ are the crystal field parameters of rank s and are related to the structure around rare earth ions. $\Xi(s,t)$ is related to the matrix elements between the two radial wave functions of 4f and the admixing levels, e.g. 5d, 5g and the energy difference between these levels. It has been suggested by Reisfeld [21] that Ξ correlates to the nephelauxetic parameter β, which indicates the degree of covalency of the R–O bond. In the present work, there is no shift in the peak wavelength of the hypersensitive transition. Hence it is observed from the above equation that $|A_{s,p}|$ alone is responsible for the decrease in Ω_2 parameter with the increase in x from 12 to 16 mol% and 16–20 mol% indicating the structural variations at these compositions.

3.2. Radiative properties

Using Judd–Ofelt intensity parameters and using the formulae given in Ref. [20], total radiative transition probabilities (A_T) and radiative lifetimes (τ_R) for the excited states, $^4G_{9/2}$, $^4G_{7/2}$, $^4G_{5/2}$, $^2H_{11/2}$, $^4F_{9/2}$, $^4F_{5/2}$ and $^4F_{3/2}$ of Nd^{3+} are estimated. The error in estimated radiative lifetimes is nearly $\pm 10\%$ for all the excited states. It is observed that the total radiative transition probabilities of all the excited states increase with the increase in covalency of the rare earth ion site, as reported earlier in other borate glasses [20]. It is observed that the variation in radiative lifetimes of most of the excited states are very less for $x=$ 16, 20 and 24 mol%. The branching ratios (β) and integrated absorption cross-sections ($\Sigma \times 10^{18}$, cm) are calculated for certain transitions. It is observed that branching ratio values are high at $x=16$ mol% and integrated absorption cross-sections are high at $x=12$ mol% for most of the transitions. These values for $x=12$ and 16 mol% are shown below.
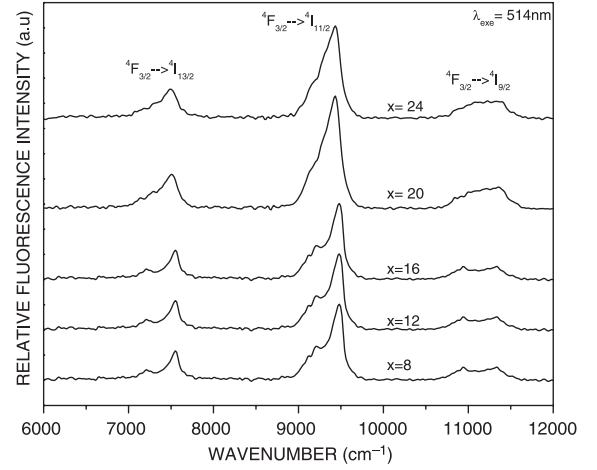

Fig. 3. Luminescence spectra of Nd^{3+} in $67B_2O_3 \cdot xLi_2O \cdot (32-x)$ Cs_2O ($x=8$, 12, 16, 20 and 24) glasses.

514 nm of Ar^{3+} laser are shown in Fig. 3. In the emission spectra, three bands $^4F_{3/2} \rightarrow ^4I_{9/2}$, $^4F_{3/2} \rightarrow ^4I_{11/2}$ and $^4F_{3/2} \rightarrow ^4I_{13/2}$ are observed at $\cong 11,350$, $\cong 9500$, and $\cong 7500$ cm^{-1}, respectively. From the spectra, it is observed that the peaks corresponding to the three transitions splits into two peaks for $x=8$, 12 and 16 mol%. There is no splitting of the peaks for $x=20$ and 24 mol%. The peak to peak separation for the three bands corresponding to the transitions, $^4F_{3/2} \rightarrow ^4I_{9/2}$, $^4F_{3/2} \rightarrow ^4I_{11/2}$ and $^4F_{3/2} \rightarrow ^4I_{13/2}$ are 380, 263 and 340 cm^{-1} and they are the same for $x=8$, 12 and 16 mol%. It indicates structural variations and the accompanying changes at $x=12$–16 and 16–20 mol% in the glass matrix. Fig. 4 shows emission spectra of Nd^{3+} ($x=$

	$^4G_{9/2} \rightarrow ^4I_{13/2}$		$^4G_{7/2} \rightarrow ^4I_{11/2}$		$^4G_{5/2} \rightarrow ^4I_{9/2}$		$^2H_{11/2} \rightarrow ^4I_{15/2}$		$^4F_{5/2} \rightarrow ^4I_{9/2}$		$^4F_{3/2} \rightarrow ^4I_{11/2}$	
	β	Σ	β	Σ	β	Σ	β	Σ	β	Σ	β	Σ
$x=12$	0.539	47.9	0.597	41.5	0.834	87.6	0.525	3.8	0.673	26.8	0.522	27.5
$x=16$	0.546	29.6	0.603	25.6	0.838	54.1	0.538	2.4	0.669	15.6	0.515	15.9

It is noticed that the transition, $^4G_{5/2} \rightarrow ^4I_{9/2}$ has higher branching ratio and integrated absorption cross-section values when compared with other transitions. $^4F_{3/2} \rightarrow ^4I_{11/2}$ transition is a potential lasing transition for Nd^{3+} ion. The calculated branching ratios of this transition are 0.537, 0.522, 0.515, 0.516 and 0.533 for $x=8$, 12, 16, 20 and 24 mol% in lithium cesium glass matrix. In the case of lithium sodium and lithium potassium mixed alkali borate glasses, the branching ratios for the above transition are in the range 0.499–0.518 and 0.491–0.552, respectively [15].

3.3. Photoluminescence spectra

The luminescence spectra of Nd^{3+} in lithium cesium mixed alkali borate glasses recorded at room temperature in the region 6000–12,000 cm^{-1}, under excitation wavelength

8 mol%) recorded at different excitation power. It is observed that the intensity of the three emission peaks and the peak splitting increase with the increase in excitation power.

The peak stimulated emission cross-sections (σ_p) are calculated using the expression given in Ref. [15] for the three transitions recorded at 100 mW and these values are presented in Table 2 along with the peak wavelengths (λ_p), effective line widths ($\Delta\lambda_{eff}$) and transition probabilities (A). The emission band, $^4F_{3/2} \rightarrow ^4I_{11/2}$ at $\cong 9500$ cm^{-1} has been considered as a potential lasing transition due to the large stimulated emission cross-section. In the present work, for $^4F_{3/2} \rightarrow ^4I_{11/2}$ transition, σ_p values are 10.87, 9.21, 5.39, 5.37 and 5.20 for $x=8$, 12, 16, 20 and 24 mol% in the glass matrix. It indicates emission cross-section decreases with the decrease in cesium content. From the present studies it
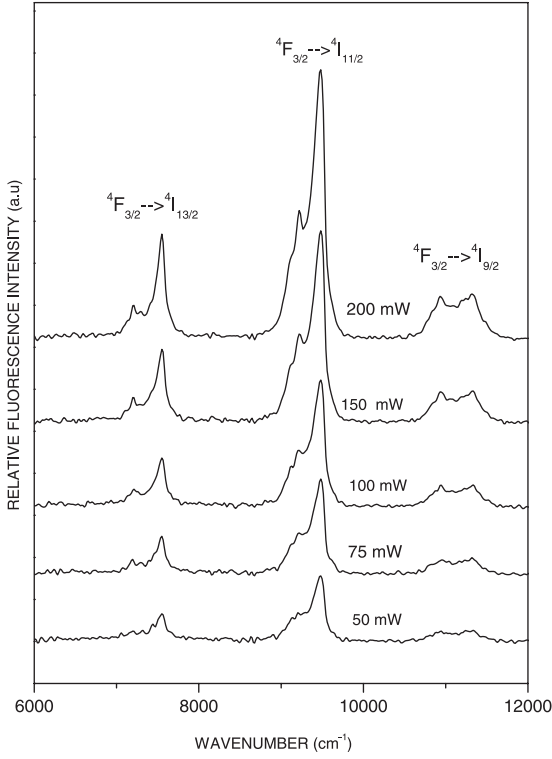
Fig. 4. Emission spectra of Nd^{3+} in $67B_2O_3 \cdot 8Li_2O \cdot 24Cs_2O$ glass at different excitation power.

can be concluded that the transition $^4F_{3/2} \rightarrow {}^4I_{11/2}$ at $x=8$ mol% in lithium cesium mixed alkali borate glass could be useful for laser excitation. The emission cross-sections for lithium sodium and lithium potassium mixed alkali borate glasses are in the range 5.38–6.16 and 4.20–8.84, respectively [15]. The variation of fluorescence intensity with x at different excitation power for the three emission transitions is shown in Fig. 5. It is observed that the fluorescence intensity increases with the increase in x up to $x=20$ mol% and further decreases indicating structural changes at $x=16$–20 and 20–24 mol%.

4. Conclusions

Among the three mixed alkali borate glasses of the type $67B_2O_3 \cdot xLi_2O \cdot (32-x)R_2O$ (where $x=8$, 12, 16, 20 and 24) (R=Na, K and Cs), Ω_2 parameter is larger in lithium cesium glass matrix at $x=12$ mol% indicating strong covalency and more asymmetry. The sum of the Judd–Ofelt intensity parameters ($\Sigma\Omega_\lambda$) is nearly equal for $x=8$ and 12 mol% and they are large indicating higher crystal field asymmetry and covalency. Similarly $\Sigma\Omega_\lambda$ is nearly equal at $x=20$ and 24 mol% and they are small indicating lower crystal field asymmetry and covalency. The spectral profiles of the hypersensitive transition are different for

Table 2
Certain fluorescence properties of Nd^{3+} doped lithium cesium mixed alkali borate glasses

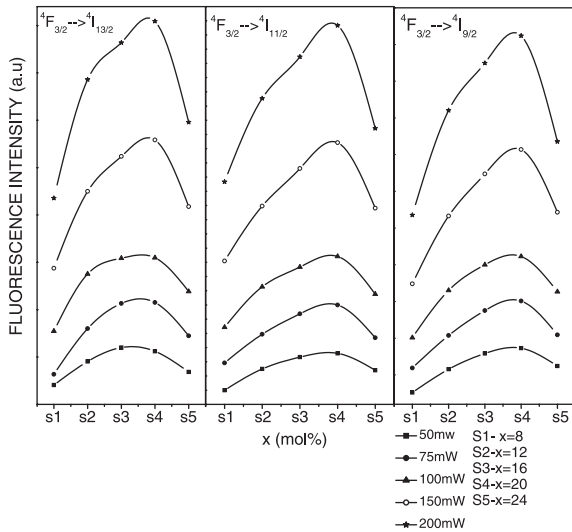| S. No	Glass	$^4F_{3/2} \rightarrow {}^4I_{13/2}$				$^4F_{3/2} \rightarrow {}^4I_{11/2}$				$^4F_{3/2} \rightarrow {}^4I_{9/2}$			
		λ_P (nm)	A_{rad} (s^{-1})	$\Delta\upsilon$ (cm^{-1})	σ_P (10^{-20} cm^2)	λ_P (nm)	A_{rad} (s^{-1})	$\Delta\upsilon$ (cm^{-1})	σ_P (10^{-20} cm^2)	λ_P (nm)	A_{rad} (s^{-1})	$\Delta\upsilon$ (cm^{-1})	σ_P (10^{-20} cm^2)
1	$x=8$	1324	1163	240	4.17	1055	5700	315	10.87	882	3702	511	2.76
2	$x=12$	1324	949	236	3.47	1055	4860	289	9.21	882	3463	517	2.56
3	$x=16$	1324	548	238	2.00	1055	2823	288	5.39	882	2088	524	1.53
4	$x=20$	1332	551	306	1.57	1060	2824	290	5.37	881	2069	418	1.89
5	$x=24$	1335	577	299	1.69	1060	2899	307	5.20	882	1942	567	1.31

Fig. 5. Variation of fluorescence intensity with x at different excitation power.

different x values in the glass matrix indicating significant differences in the crystal field asymmetries. The Stark splitting of the $^4I_{9/2} \to {}^4G_{5/2} + {}^2G_{7/2}$ transition is not resolved for $x = 8$ mol%. There is clear splitting for $x = 12$ and 16 mol%. For $x = 20$ and 24 mol% the splitting is decreased and the relative intensities of the components changed, so that the splitting is hidden by the inhomogeneous broadening. It indicates structural changes at $x = 16$–20 mol% and at $x = 20$–24 mol%.

Radiative lifetimes of all the excited states of Nd^{3+} ion are greatest at $x = 20$ and 24 mol% and the variation in lifetimes of the most of the excited states are very less for $x = 16$, 20 and 24 mol%. Among various transitions, $^4G_{5/2} \to {}^4I_{9/2}$ has highest branching ratio and integrated absorption cross-section values. The calculated branching ratio of the transition, $^4F_{3/2} \to {}^4I_{11/2}$ (potential lasing transition for Nd^{3+} ion) is more at $x = 8$ mol% in lithium cesium glass matrix. The peaks corresponding to three emission transitions, $^4F_{3/2} \to {}^4I_{9/2}$, $^4F_{3/2} \to {}^4I_{11/2}$ and $^4F_{3/2} \to {}^4I_{13/2}$ splits into two peaks for $x = 8$, 12 and 16 mol% and there is no splitting of the peaks for $x = 20$ and 24 mol%. The peak to peak separation for the three bands are 380, 263 and 340 cm^{-1} and they are the same for $x = 8$, 12 and 16 mol%. It indicates structural variations and the accompanying changes at $x = 12$–16 and 16–20 mol% in the glass matrix. The emission cross-sections decrease with the decrease in cesium content. From the present work, it can be concluded that the transition $^4F_{3/2} \to {}^4I_{11/2}$ at $x = 8$ mol% in lithium cesium mixed alkali borate glass could be useful for laser excitation.

References

[1] A. Speghini, M. Peruffo, M. Casarim, D. Ajo, M. Bettinelli, J. Alloys Compd. 300–301 (2000) 114.

[2] M.B. Saisudha, J. Ramakrishna, Phys. Rev. B 53 (10) (1996) 6186.

[3] W. Sopp, J. Klearebezem, H.W. den Hartog, J. Non-Cryst. Solids 93 (1987) 142.

[4] N.A. Saraf, A.A. Ahmed, A.F. Abbas, Phys. Chem. Glasses 39 (2) (1998) 76.

[5] G. Ajith Kumar, P.R. Biju, N.V. Unnikrishnan, Phys. Chem. Glasses 40 (4) (1999) 219.

[6] M. Naftaly, A. Jha, J. Appl. Phys. 87 (5) (2000) 2098.

[7] K. Lu, N.K. Dutta, J. Appl. Phys. 89 (6) (2001) 3079.

[8] M. Zambelli, A. Speghini, G. Ingietto, C. Locatelli, M. Bettinelli, F. Vetrone, J.C. Boyer, J.A. Capobianco, Opt. Mater. 25 (2004) 215.

[9] H. Li, L. Li, J.D. Vienna, M. Qian, Z. Wang, J.G. Darab, D.K. Peeler, J. Non-Cryst. Solids 278 (2000) 35.

[10] V. Lavin, I. Iparraguirre, J. Azkargorta, A. Mendioroz, J. Gonzalez-Platas, R. Balda, J. Fernandez, Opt. Mater. 25 (2004) 201.

[11] B.R. Judd, Phys. Rev. B 127 (1962) 750.

[12] G.S. Ofelt, J. Chem. Phys. 37 (1962) 511.

[13] P. Maass, A. Bunde, M.D. Ingram, Phys. Rev. Lett. 68 (1992) 3064.

[14] D.E. Day, J. Non-Cryst. Solids 21 (1976) 343.

[15] Y.C. Ratnakaram, A. Vijaya Kumar, D. Tirupathi Naidu, R.P.S Chakradhar, K.P. Ramesh, J. Lumin. 110 (1–2) (2004) 63.

[16] S. Tanabe, T. Ohyagi, N. Soga, T. Hanada, Phys. Rev. B 46 (1992) 3305.

[17] E.W.J.L. Oomen, A.M.A. Van Dongen, J. Non-Cryst. Solids 111 (1989) 205.

[18] X. Zou, H. Toratani, J. Non-Cryst. Solids 195 (1996) 113.

[19] B.R. Judd, Proc. Phys. Soc. Lond., Ser. A 69 (1956) 157.

[20] H. Takebe, K. Morinaga, T. Izumitani, J. Non-Cryst. Solids 178 (1994) 58.

[21] R. Reisfeld, Struct. Bond. 22 (1975) 123.

[22] K.A. Gschncidner, L. Eyring (Eds.), Excited State Phenomena in Vitreous Materials Hand book on the Physics and Chemistry of Rare Earths vol. 9 (1998) (chapter 58, Amsterdam).